scientific reports

Check for updates

OPEN

A natural coumarin, benjaminin, suppresses proliferation and migration and induces apoptosis in MCF-7 breast cancer cells

Melissa Kilus[1], Shaari Daud[3], Nurhuda Mohamad Ansor[1], Julia Joseph[4], Gwendoline Cheng Lian Ee[5] & Nozlena Abdul Samad[1,2]✉

Breast cancer remains the leading cause of cancer-related mortality in women, highlighting the need for selective and effective therapeutics. Conventional chemotherapies are often limited by off-target toxicity, prompting interest in natural products, including coumarins from *Calophyllum* species. Benjaminin, a novel coumarin, has demonstrated cytotoxicity in multiple cancer models, yet its effects in breast cancer remain unexplored. Here, we evaluated benjaminin in MCF-7 (tumorigenic) and MCF-10A (non-tumorigenic) breast cells. Benjaminin exhibited moderate but highly selective cytotoxicity toward MCF-7 cells while sparing normal epithelial cells. Mechanistic analyses revealed pronounced G1-phase arrest and apoptotic induction, confirmed by propidium iodide and Annexin V-FITC staining. Protein array profiling indicated upregulation of DR6 and Bax, consistent with activation of a non-classical extrinsic apoptotic pathway with mitochondrial priming. Functional assays demonstrated impaired migration and spreading, associated with lamellipodia loss and cytoskeletal disorganization, consistent with disruption of pathways involving cyclin D1–paxillin–Rac1–Arp2/3 signaling. These findings indicate that benjaminin may exert coordinated, multi-level anticancer effects, potentially connecting cyclin D1 downregulation with cell-cycle arrest, cytoskeletal dysregulation, apoptotic activation, and reduced migratory behavior. This study provides the first integrated mechanistic characterization of benjaminin in breast cancer cells and supports further investigation in additional subtypes, in vivo models, and pathway-specific analyses.

Keywords Benjaminin, Breast cancer, *Calophyllum*, Cytotoxicity, Migration, Cell cycle arrest

Breast cancer continues to pose a severe global health challenge, with Asia recording the highest incidence, mortality, and prevalence worldwide. In 2022, Southeast Asia as a whole recorded 14.7 new cases per 100,000 population. In Malaysia, breast cancer is estimated at 8,371 new cases, making breast cancer the most commonly diagnosed cancer in the country. Experts project that global new cases could exceed three million, with up to one million potential deaths. These trends highlight the urgent need for effective prevention strategies and therapeutic interventions[1,2]. Studies indicate that recurrent tumors can be more aggressive than the primary tumor, underscoring the need for therapeutic strategies that also inhibit migration, even in early-stage disease[3].

At the cellular level, breast cancer progression is driven by dysregulated cell cycle control and apoptosis evasion[4]. Cyclin D1 and p53 are key regulatory proteins, and elevated cyclin D1 expression is associated with uncontrolled proliferation and enhanced cytoskeletal remodeling, which contributes to cell migration and invasion[5–7], highlighting its potential as a target for strategies that simultaneously inhibit proliferation and migration.

[1]Department of Toxicology, Pusat Kanser Tun Abdullah Ahmad Badawi, Universiti Sains Malaysia, 13200 Kepala Batas, Pulau Pinang, Malaysia. [2]Breast Cancer Translational Research Program (BCTRP@PKTAAB), Pusat Kanser Tun Abdullah Ahmad Badawi, Universiti Sains Malaysia, 13200 Kepala Batas, Pulau Pinang, Malaysia. [3]Faculty of Applied Sciences, Universiti Teknologi MARA (Cawangan Pahang), Bandar Jengka, 26400 Bandar Tun Razak, Pahang, Malaysia. [4]Faculty of Medicine and Health Sciences, Universiti Malaysia Sabah, Jalan UMS, 88400 Kota Kinabalu, Sabah, Malaysia. [5]Department of Chemistry, Faculty of Science, Universiti Putra Malaysia, 43400UPM, Serdang, Selangor, Malaysia. ✉email: nozlena@usm.my

Chemotherapeutic agents such as doxorubicin are commonly used as first-line treatments for cancers, including breast cancer. However, their clinical use is limited by off-target effects, which may lead to both acute and long-term adverse outcomes[8]. These limitations have stimulated interest in natural product-based therapeutics, which can offer selective anticancer activity while maintaining low toxicity, high efficacy, and better biocompatibility[9]. In this context, *Calophyllum* species are a significant source of bioactive compounds, and their traditional use in treating diseases suggests good bioavailability and safety[10]. Many have yielded multiple bioactive compounds exhibiting promising anticancer activity[11,12], with coumarins representing one of the major compound classes. Notable examples with anticancer activity include GUT-70[13] and mammea-type coumarins[14], which have demonstrated cytotoxic effects against cancer cells. Structure–activity analyses indicate that prenyl substitution at the C-6 position is frequently observed among coumarins with reported anticancer activity[11]. Consistent with this observation, the coumarin benjaminin, which retains this structural feature, has shown broad cytotoxicity across several cancer cell lines[15,16]. Yet, its effects on breast cancer cell proliferation, apoptosis, and migration remain poorly understood.

Therefore, the present study aims to address this gap by evaluating the anticancer activity of benjaminin and investigating its underlying mechanisms. By providing selectivity and mechanistic insights into its activity, this work advances understanding of coumarin-based therapeutics and may inform the development of safer, more effective interventions for patients with breast cancer. These findings have potential relevance for translational research, offering a foundation for preclinical evaluation and eventual clinical applications.

Material and methods

Materials

The human breast adenocarcinoma cell line, Michigan Cancer Foundation-7 (MCF-7), and the immortalized normal human mammary epithelial cell line, Michigan Cancer Foundation-10A (MCF-10A), were obtained from the American Type Culture Collection (ATCC, Manassas, VA, USA). Dulbecco's Modified Eagle Medium/Ham's F-12 Nutrient Mixture (DMEM/F-12), 0.25% trypsin/EDTA, and hydrocortisone were obtained from Nacalai Tesque (Japan). Dulbecco's Modified Eagle Medium (DMEM) and the Annexin V-FITC Apoptosis Detection Kit were obtained from Elabscience (USA). Penicillin–streptomycin, dimethyl sulfoxide (DMSO), phosphate-buffered saline (PBS) tablets, fetal bovine serum (FBS), Triton X-100, and thiazolyl blue tetrazolium bromide (MTT), and Fluoroshield with 4′,6-diamidino-2-phenylindole (DAPI) mounting solution were purchased from Sigma-Aldrich (USA). Mitomycin C was obtained from Roche (Germany). RNase A, horse serum, epidermal growth factor (EGF), insulin, and phalloidin Alexa Fluor 568 were purchased from Thermo Fisher Scientific (USA). Paraformaldehyde (PFA) was obtained from GE Chemicals Supplies (Malaysia). Absolute ethanol was obtained from System Chemicals (Malaysia). Bovine serum albumin (BSA) was purchased from TOCRIS (UK). Primary antibody against α-tubulin (DM1A, mouse monoclonal antibody) was purchased from Cell Signaling Technology (USA), and Alexa Fluor 488-conjugated secondary antibodies were purchased from Abcam (UK). Fibronectin was purchased from R&D Systems (USA). RayBio® Human Apoptosis Array G1 kit was purchased from Raybiotech (USA).

Plant compound

Benjaminin ($C_{25}H_{36}O_6$), obtained as a yellowish oil[16], was kindly provided by Dr. Shaari Daud from Universiti Teknologi MARA (UiTM) Pahang, Malaysia. The compound's purity had been verified by the provider using ^{1}H NMR spectroscopy (Supplementary Information 1). Benjaminin was dissolved in DMSO to prepare a 40 mg/mL stock solution and stored at – 4 °C until further use. Working concentrations were freshly prepared prior to each experiment.

Cell culture

MCF-7 cells were grown in DMEM supplemented with 10% FBS and 1% of 100x penicillin–streptomycin solution. MCF-10A cells were grown in DMEM/F-12 supplemented with 5% horse serum, 0.02% of 100 µg/ml EGF, 0.25% of 10 µg/ml insulin, 0.05% of 1 mg/ml hydrocortisone, and 1% of 100x penicillin–streptomycin solution. All cells were incubated at 37°C in a humidified incubator with 5% CO_2. Cultures at approximately 80% confluence were detached using trypsin and used for experiments.

Cell viability assay

MCF-7 and MCF-10A cells seeded in a 96-well plate at density of 1×10^4 cells/well were incubated overnight to adhere. Then, media containing various concentrations of benjaminin up to 400 µg/ml were added and followed with incubation for 24, 48, and 72 h for MCF-7, and 24 h for MCF10A. Equivalent volume of DMSO (1% v/v) was used as vehicle control. Blank wells containing only media was used as background control. At the end of each timepoint, media from each well was replaced with fresh media containing 10% of 5 mg/ml MTT reagent. The plate was protected from light using aluminium foil wrap and re-incubated for 4 h. After that, MTT medium was replaced with 100 µl of DMSO while protected from light to dissolve the formazan crystals. Finally, the absorbance of each well was measured at 570 nm with 620 nm reference wavelength (ELx808 Absorbance Reader, Biotek). The cell viability was calculated according to the formula below:

$$\text{Cell viability} = \frac{\text{absorbance of treated cell}}{\text{absorbance of control}} \times 100\%$$

A concentration–response curve for cell viability was generated using Microsoft Excel 2016, and IC_{50} values were derived from the plotted graph.

Selectivity of compound was assessed using the following formula:

$$\text{Selectivity index(S.I)} = \frac{Normal\ cell\ IC50}{Cancer\ cell\ IC50}$$

Morphology assay

Approximately 3×10^5 MCF-7 cells were seeded in 6-well plate and incubated adhere. Then, media containing benjaminin or equivalent volume of DMSO (0.1% v/v) were added to make a final concentration based on the IC_{50} derived from MTT assay. After 24 h treatment, photomicrographs of cells were taken using inverted microscope (Olympus IX51) at 400 × magnification.

Cell cycle assay

Approximately 5×10^5 MCF-7 cells in T25 flask were starved in serum-free medium for 24 h to synchronise all cells to G1. Then, the medium was replaced with a fresh one containing benjaminin at IC_{50} final concentration. Equivalent volume of DMSO (0.1% v/v) was used as control. After 24 h incubation, the cells were detached by trypsinisation and washed in PBS. Cell pellet was then fixed in 5 ml cold 70% ethanol added dropwise with vortexing and stored at -4 °C until further use. Fixed cells were washed in PBS, resuspended, and incubated in 1 ml staining solution containing 0.1 µl Triton X and 0.5 µl RNase in PBS for 30 min at room temperature. Then, 25 µl of 1 mg/ml propidium iodide solution was added and the solution incubated for 10 min at room temperature in the dark. Cell cycle profile was determined using flow cytometer (BD FACSCalibur) and analysed using ModFit software.

Annexin V apoptosis assay

Approximately 5×10^5 cells were seeded in T25 flask and incubated overnight to adhere. Then, the cells were subjected to 24 h treatment with IC_{50} value of benjaminin or equivalent volume of DMSO (0.1% v/v). After that, detection of apoptotic and/or necrotic cells was carried out using Annexin V-FITC Apoptosis Detection kit according to the manufacturer's protocol. Briefly, cells were detached by trypsinisation, washed in PBS, adjusted to 1×10^5 cells, and resuspended in 500 µl of cold 1X binding buffer. Next, 5 µl annexin-V and 5 µl propidium iodide were mixed in and incubated at room temperature in the dark for 30 min. The cells were kept on ice and protected from light before the flow cytometry analysis (BD FACSCalibur).

Apoptosis protein array

Approximately 5×10^5 MCF-7 cells were seeded in T25 flasks and incubated overnight to adhere. Cells were then treated for 24 h with the IC_{50} concentration of benjaminin or equivalent volume of DMSO (0.1% v/v). After treatment, total protein was extracted using the lysis buffer provided in the RayBiotech Apoptosis Array Kit. For each treatment condition, lysates from two independent flasks were pooled to ensure sufficient protein yield and reduce variability. Pooled protein lysates were applied to the array according to the manufacturer's instructions, and slides were scanned using an Agilent G2505C microarray scanner (Genomax, Malaysia). Signal intensities were analyzed using the manufacturer's template (AAH-APO-G1) and fold changes were calculated in Microsoft Excel 2016. Fold change values of 1 or − 1 were considered indicative of no change, whereas values > 1.5 were interpreted as upregulation and values < − 1.5 as downregulation[17,18].

Wound healing assay

MCF-7 cells were grown in 6-well plate until it forms a monolayer. Then, the growth media was replaced with media containing 4 µg/ml mitomycin C for 2 h to inhibit proliferation. A wound gap was created by 'scratching' the monolayer using sterile yellow pipette tip held vertically and dragged across from the top to the bottom of the well with moderate and consistent speed and pressure. Detached cells and debris were washed off with PBS to ensure the gap is clear of cells. At this point, at least six consistent locations along the wound areas were photographed using phase-contrast microscope at 40 × magnification to represent scratch area at 0-h. Then, media containing benjaminin at IC_{50} concentration was added. Equivalent volume of DMSO (0.1% v/v) was used as control. Photomicrographs were taken at subsequent 12 and 24 h. All images were analysed using Fiji (ImageJ) and data was presented as square micrometer area of scratch. Percentage of wound closure was calculated using the following formula:

$$\%\ \text{wound closure} = \frac{area\ at\ 0\ hour - area\ at\ 12\ or\ 24\ hour}{area\ at\ 0\ hour} \times 100\%$$

Cell spreading assay

Cell spreading assay was carried out as previously described[19]. Briefly, 5×10^4 MCF-7 cells were seeded into 24-well plates and incubated overnight to allow adherence. Cells were then treated with the IC_{50} concentration of benjaminin or an equivalent volume of DMSO (0.1% v/v) as a control for 24 h. Following treatment, cells were trypsinized and replated onto 13 mm coverslips coated with fibronectin (1:40 dilution in PBS). Replated cells were allowed to spread for 30 min and 1 h. Cells were fixed with 4% paraformaldehyde in PBS and permeabilized with 0.1% Triton X-100. After blocking with 1% BSA in PBS for 30 min, cells were incubated with primary antibody α-tubulin (DM1A) mouse mAb (1:500) for 30 min at room temperature. Cells were then washed three times with PBS and incubated with Alexa Fluor 488-conjugated secondary antibody (1:500) and phalloidin Alexa Fluor 568 (1:200) for 30 min. All antibody and phalloidin dilutions were freshly prepared in deionized water immediately prior to use and applied for a short duration to preserve antibody functionality while minimizing potential buffer interference during incubation[20,21]. Following three PBS washes and a final rinse in deionized water, coverslips were mounted using Fluoroshield with DAPI. Fluorescent images of single cells were

captured using an Olympus BX53 microscope equipped with an Olympus DP72 camera. Cell spreading area and circularity were quantified using Fiji software (ImageJ).

Statistical analysis

Data are presented as mean ± SD from three independent biological replicates, unless otherwise stated. Statistical assumptions were assessed using the Shapiro–Wilk test for normality and Levene's test for homogeneity of variances. Comparisons between two groups were conducted using Student's *t*-test. For comparisons among multiple groups, one-way ANOVA followed by Dunnett's post hoc test was applied to compare treatment groups with the control. A p value < 0.05 was considered statistically significant. All analyses were performed using SPSS version 31 (IBM Corp., Armonk, NY, USA).

Results

Benjaminin exhibits selective cytotoxic effects on MCF-7 cells

As depicted in Fig. 1(a), MTT results revealed a time- and concentration-dependent cytotoxic activity against MCF-7 cells, achieving IC_{50} values of 45 µg/ml, 35 µg/ml, and 33 µg/ml for 24, 48, and 72 h treatment, respectively. In contrast doxorubicin produced greater cytotoxic effects, with IC_{50} values of 0.78 µg/ml, 0.71 µg/ml, and 0.63 µg/ml for the three timepoints, respectively (Fig. 1(b)). Analysis of selectivity depicted in Fig. 1(c) indicated the viability of MCF-10A cells remained well above 90% for all concentrations of benjaminin. This gives an IC_{50} of > 400 µg/ml, which translated to an excellent S.I of at least 8.8.

Benjaminin induced G1 arrest and apoptotic death in MCF-7 cells

Assessment of cell morphology following treatment with IC_{50} of benjaminin provided indication of apoptotic cell death. As annotated in Fig. 2, both benjaminin and doxorubicin treatments produced reduction in cell density as well as increase in rounded and detached cells relative to DMSO control. However, the morphology of surviving cells differed between the two treatments, where cell lamellipodia is only inhibited in benjaminin samples.

The effects of treatments on MCF-7 cell cycle progression are shown in Fig. 3. Benjaminin treatment induced pronounced G_1-phase arrest compared to the DMSO control, with a significant increase in the G_1 population ($p < 0.001$), a reduction in S-phase cells ($p = 0.005$), and a significant increase in G_2/M-phase cells ($p = 0.014$). These effects were comparable to those observed with doxorubicin, which also caused a significant increase in G_1-phase cells ($p < 0.001$), a decrease in S-phase cells ($p < 0.001$), and no significant change in G_2/M-phase cells ($p = 0.108$).

The results from annexin V apoptosis assay are presented in Fig. 4(a), confirming apoptosis induction in benjaminin-treated MCF-7 cells. Benjaminin treatment caused a significant increase in both early ($p = 0.045$) and late ($p = 0.002$) apoptotic populations, with concurrent reduction in the live cell population ($p < 0.021$).

Apoptotic protein array analysis revealed modulation of six apoptotic proteins (Fig. 4(b)). Among the 43 apoptotic proteins included in the kit (Supplementary Information 2), DR6 and caspase-8 were upregulated, indicating activation of extrinsic apoptotic signalling, while caspase-3 upregulation confirmed execution of apoptosis. Bax increased, but cytochrome c remained unchanged, suggesting partial intrinsic pathway activation. No significant changes were observed in other death receptors or their ligands (Fas, FasL, TRAIL, TRAILR) or inhibitory proteins (IGFBPs), indicating caspase-8 activation independent of surface receptor engagement. Anti-apoptotic Bcl-w and HSP27 were elevated, reflecting compensatory survival and stress response, whereas Livin was downregulated, shifting the balance toward apoptosis. p53 levels remained unchanged, suggesting a p53-independent mechanism.

Benjaminin impaired migration and spreading of MCF-7 cells

Wound healing assays (Fig. 5 (a-c)) showed that both benjaminin and doxorubicin suppressed gap closure. Benjaminin exhibited effects comparable to doxorubicin as early as 12 h, which persisted through 24 h. In DMSO controls, denuded areas progressively closed with significant reductions between time points ($p < 0.001$). In contrast, both benjaminin and doxorubicin treatments showed no significant closure between consecutive intervals ($p > 0.05$). Consequently, the rate of gap closure was significantly reduced at 12 h for benjaminin ($p = 0.004$) and doxorubicin ($p = 0.021$) relative to control, with effects maintained at 24 h (benjaminin $p < 0.001$; doxorubicin $p = 0.002$).

In addition to inhibiting migration, benjaminin significantly reduced cell spreading, as indicated by smaller cell areas at 30 min ($p < 0.001$) and 60 min ($p = 0.011$) compared with DMSO control (Fig. 6 (a-d)). Cell circularity, however, was unaffected (30 min, $p = 0.288$; 60 min, $p = 0.168$). In contrast, doxorubicin had little effect on cell area (30 min, $p = 0.854$; 60 min, $p = 0.662$) but markedly decreased circularity (30 min, $p = 0.021$; 60 min, $p < 0.001$).

Discussion

Recent advances in anticancer research increasingly prioritize tumour-selective mechanisms over indiscriminate cytotoxicity. While agents such as doxorubicin remain clinically effective[22], their lack of selectivity results in damage to normal proliferative tissues, including the skin, gastrointestinal epithelium, and hair follicles[23]. Long-term complications, particularly cardiotoxicity, further limit their therapeutic utility[24]. These challenges underscore the need for alternative strategies that suppress tumour growth while minimizing off-target toxicity. Natural metabolites from *Calophyllum* species have emerged as promising anticancer candidates, including the novel coumarin benjaminin[12]. However, its specific therapeutic potential in breast cancer remains insufficiently

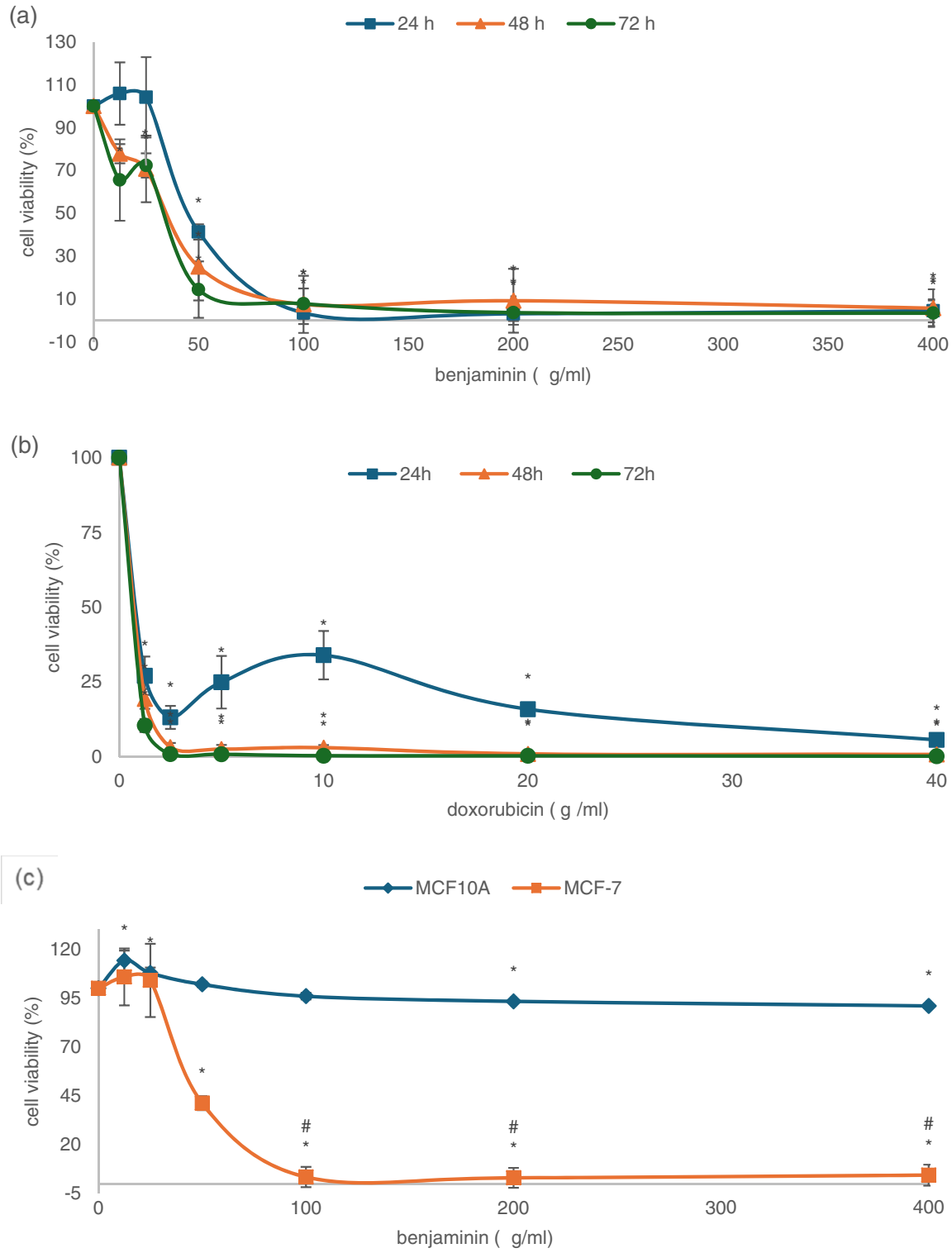

Fig. 1. Dose–response effects of benjaminin and doxorubicin on cell viability. Benjaminin exhibited a time- and concentration-dependent reduction in MCF-7 cell viability, whereas doxorubicin showed a more potent cytotoxic effect. No cytotoxicity was detected in MCF-10A cells, indicating selective activity of benjaminin toward cancerous cells. (**a**) MCF-7 cells treated with benjaminin (12.5–400 µg/mL) for up to 72 h. (**b**) MCF-7 cells treated with doxorubicin (1.25–40 µg/mL) for up to 72 h. (**c**) MCF-10A cells treated with benjaminin (12.5–400 µg/mL) for 24 h. Data represent three biological replicates (n = 3). Statistical significance was determined using Student's t-test for panels (**a**) and (**b**), and one-way ANOVA followed by Dunnett post-hoc test for panel (**c**). *P < 0.05 versus DMSO control; #P < 0.05, MCF-7 versus MCF-10A at the same concentration.

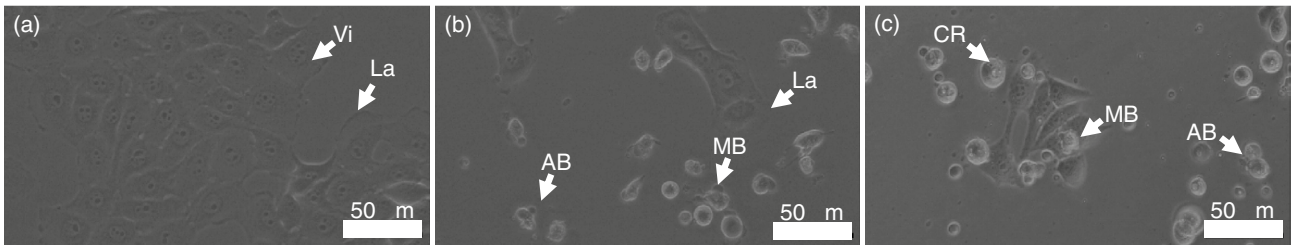

Fig. 2. Representative micrographs of MCF-7 cells after 24-h treatment. DMSO-treated cells are normal and attached with visible lamellipodia. Doxorubicin and benjaminin reduced cell density and increased rounded cells, membrane blebbing, and apoptotic bodies; lamellipodia persist with doxorubicin but are absent in benjaminin-treated cells. (**a**) 0.1% DMSO, (**b**) doxorubicin (IC_{50}), (**c**) benjaminin (IC_{50}). Abbreviations: Vi: viable cell; La: lamellipodium; MB: membrane blebbing; CR: cell rounding; AB: apoptotic body. Images are taken at 400 × magnification using inverted microscope. Scale bar: 50 µm.

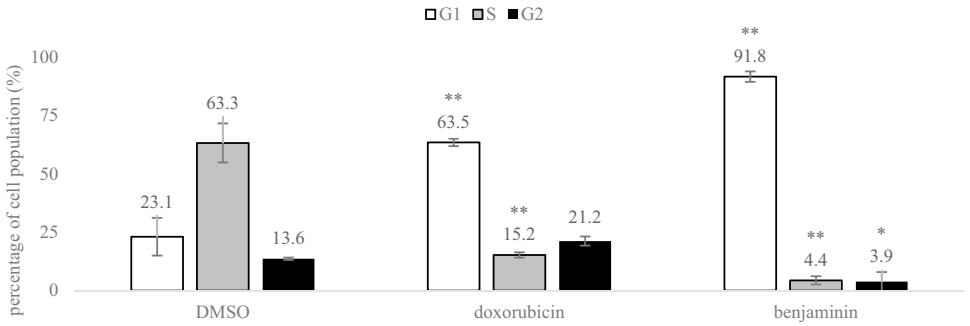

Fig. 3. Effects on MCF-7 cell cycle following 24 h of treatment. Both doxorubicin and benjaminin induced significant G_1-phase arrest, accompanied by a corresponding decrease in S-phase cells. Bar charts show the percentage of cells in different cell cycle phases after treatment with 0.1% DMSO (control), doxorubicin (IC_{50}), or benjaminin (IC_{50}). Data are presented as mean ± SD from three independent biological replicates (n = 3). Statistical significance was determined using Student's t-test. *P < 0.05, **P < 0.001.

defined. To address this gap, the present study evaluated benjaminin in MCF-7 (tumorigenic) and MCF-10A (non-tumorigenic) breast cell lines[25,26], using the 24-h IC_{50} concentration to evaluate early cellular responses.

The present in vitro findings position benjaminin as a compound exerting coordinated antiproliferative, pro-apoptotic, and antimigratory effects in breast cancer cells. However, as the study was limited to a luminal A, ER-positive model, broader subtype applicability remains to be determined. In MCF-7 cells, benjaminin demonstrated moderate cytotoxic activity and was less potent than doxorubicin. According to established classification criteria for pure compounds, IC_{50} values < 4 µg/mL are considered potent, whereas values > 100 µg/mL are classified as inactive[27]. Importantly, benjaminin did not exhibit detectable toxicity in MCF-10A cells under the conditions tested, suggesting a degree of cancer cell selectivity consistent with reports on other coumarin derivatives[28].

The comparable sensitivity observed in MCF-7 and previously studied SNU-1 cells may reflect shared molecular characteristics, notably functional TP53 and cyclin D1 overexpression[6,15,29,30]. These features may contribute to responsiveness to benjaminin. Supporting this, benjaminin inhibited the G1-to-S phase transition within 24 h of exposure, highlighting the G1 phase as a primary cellular target. While G1 arrest is often linked to DNA damage–induced activation of the p53-dependent checkpoint pathway[31–33], no significant changes in p53, p21, or p27 expression were observed, suggesting that classical p53–p21–mediated CDK inhibition was likely not engaged[34]. These findings are consistent with a possible modulation of cyclin D1–dependent pathways, in line with the reliance of MCF-7 cells on the cyclin D1–Rb regulatory axis[30,35] and their lack of endogenous p16 expression[36]. However, direct effects on cyclin D1 expression or activity were not measured in this study, and its involvement remains inferential.

Beyond its role in cell-cycle progression, cyclin D1 has been implicated in cytoskeletal regulation through the paxillin–Rac1–Arp2/3 signalling axis, where cytoplasmic cyclin D1 facilitates Rac1 activation and promotes Arp2/3-mediated actin nucleation and remodelling[37–39]. Consistent with this reported biology, benjaminin-treated cells exhibited impaired cytoskeletal organisation and migratory behaviour, characterized by reduced spreading, increased circularity, and absence of lamellipodia[7]. These phenotypic changes resemble features associated with disrupted Rac1–Arp2/3-mediated actin dynamics. This may suggest a possible involvement of cyclin D1-associated cytoskeletal signalling, although the pathway was not directly examined and causality cannot be established from the present data.

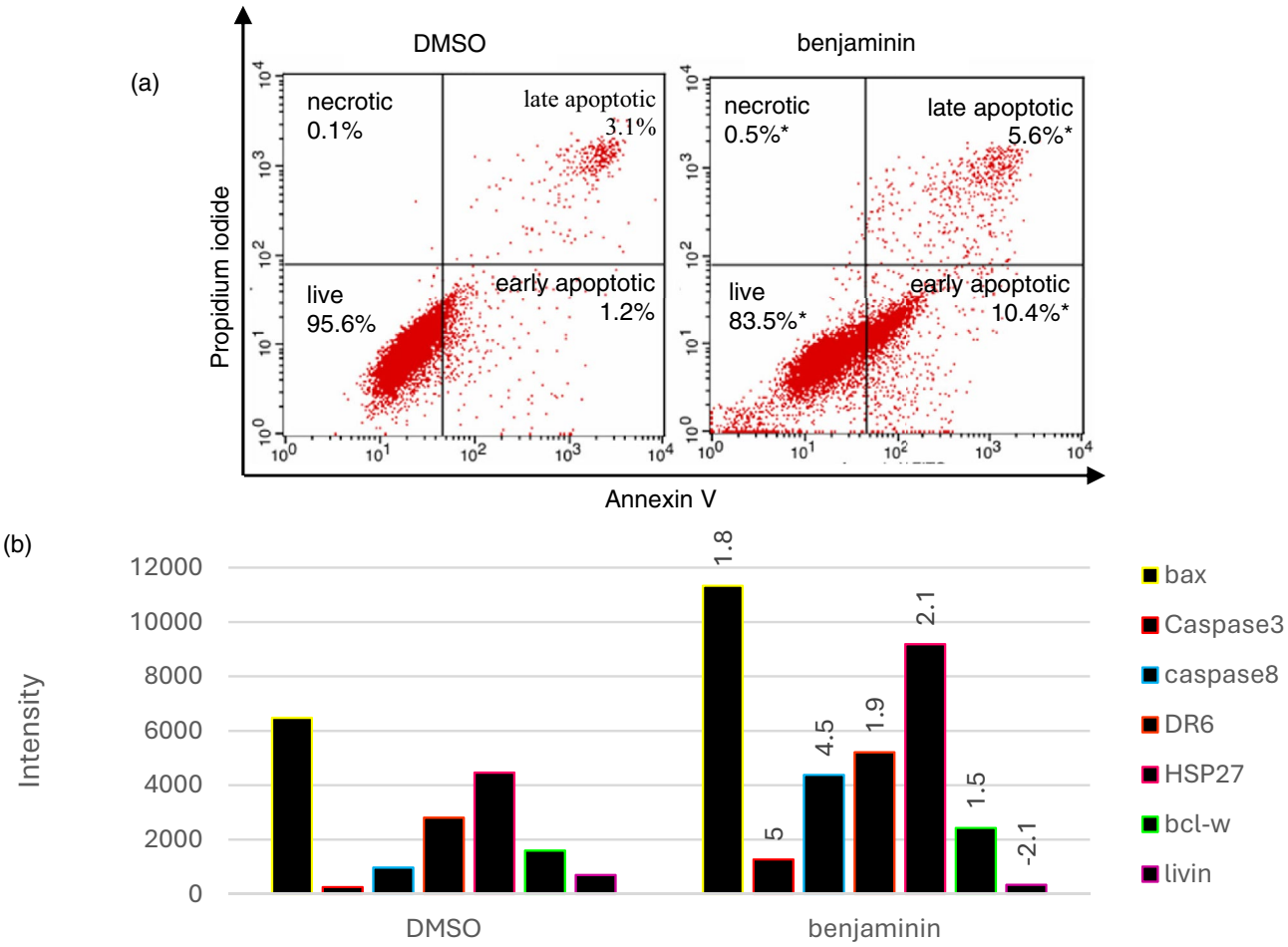

Fig. 4. Effects of benjaminin on apoptosis activation and apoptotic protein levels following 24 h of treatment with 0.1% DMSO (control) or benjaminin (IC_{50}). Benjaminin increased the proportion of apoptotic cells and modulated apoptotic protein expression. (**a**) Representative cytograms showing cell distribution across apoptotic stages. (**b**) Fold changes in apoptotic protein signal intensity relative to DMSO; lysates were pooled from two independent experiments. Data in (**a**) are mean ± SD of three biological replicates (n = 3). Statistical significance was determined using Student's t-test. *P < 0.05, **P < 0.001.

In addition, apoptotic activation occurred concurrently with G1 arrest. Flow cytometric analysis demonstrated increased apoptotic populations, accompanied by elevated effector caspase activity. At 24 h, apoptosis appeared to be initiated predominantly via the extrinsic pathway, as evidenced by increased caspase-8 expression[40]. However, no upregulation of Fas/FasL was observed, consistent with the low basal Fas expression in MCF-7 cells[41]. Instead, DR6 was markedly upregulated in parallel with increased Bax expression. These findings suggest activation of a non-classical extrinsic pathway, with potential crosstalk to the mitochondrial pathway via a DR6–Bax axis[42] . Despite incomplete intrinsic pathway activation at this early timepoint, the observed mitochondrial priming indicates mitochondrial priming, which could facilitate subsequent intrinsic pathway engagement upon prolonged exposure.

Collectively, these in vitro findings show that benjaminin is associated with G1-phase accumulation, apoptosis, and altered cytoskeletal organisation in MCF-7 cells. As all observations were derived from short-term exposure at the 24-h IC_{50}, longer-term adaptive responses and clinical relevance remain to be established. While the observed phenotypes may overlap with processes regulated by cyclin D1-associated signalling and Rac1–Arp2/3-mediated cytoskeletal dynamics, these pathways were not directly assessed and therefore remain hypothetical. These proposed mechanisms require validation through targeted approaches, including Western blotting and pathway-specific activity assays. Further studies in more aggressive breast cancer models, such as MDA-MB-231, and in vivo systems will be essential to evaluate translational potential. Notably, the observed effects in the absence of detectable p53 pathway activation may suggest relevance in tumours resistant to classical apoptotic pathways.

Conclusion

In conclusion, these in vitro findings show that benjaminin inhibits proliferation and migration while inducing apoptosis in MCF-7 breast cancer cells with minimal toxicity toward non-tumorigenic MCF-10A mammary

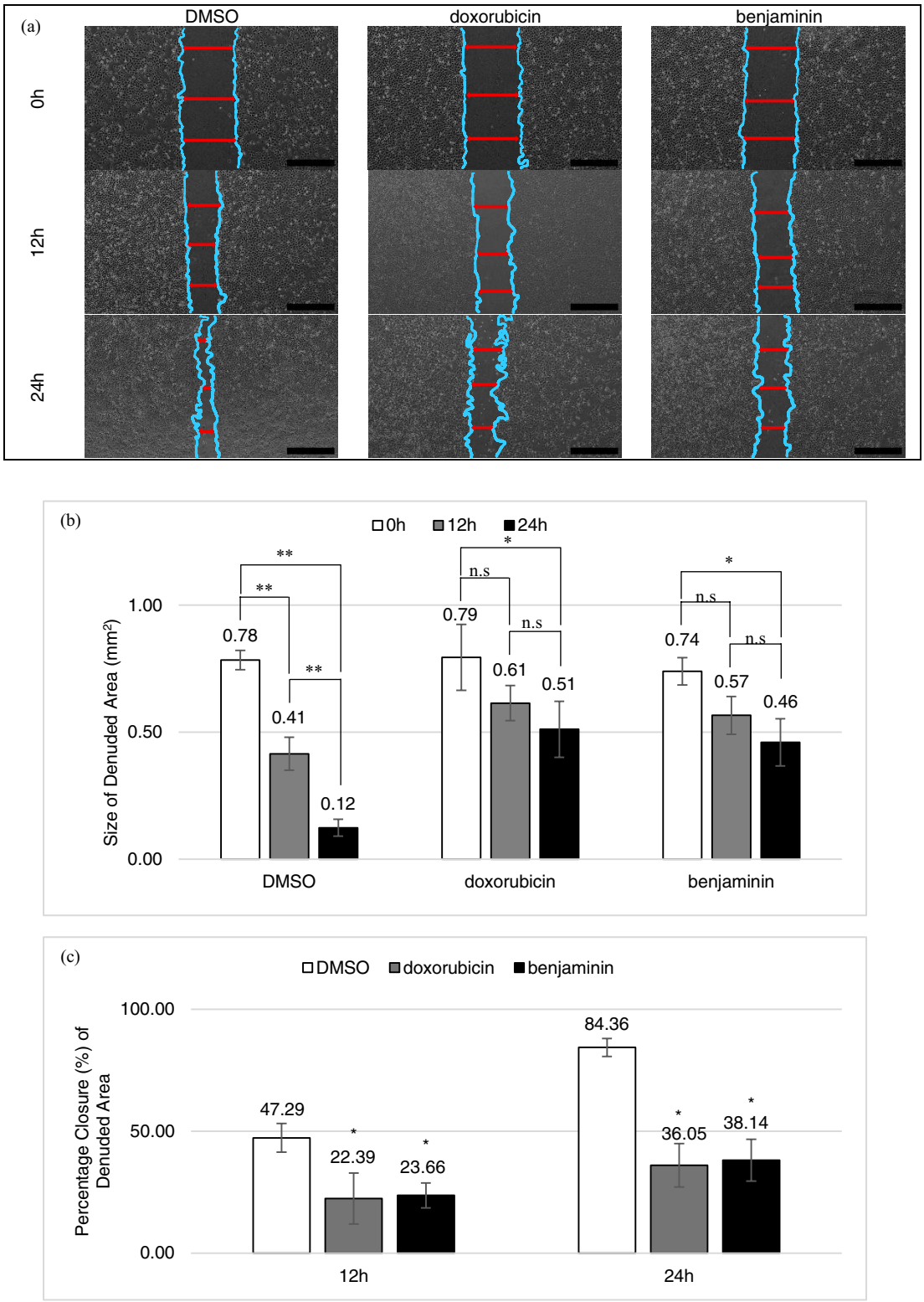

Fig. 5. Effects of treatment on MCF-7 cell migration. Benjaminin inhibited wound closure to a degree comparable to doxorubicin. Whereas DMSO-treated cells exhibited progressive closure over time, benjaminin- and doxorubicin-treated cells showed no significant changes between consecutive time points, indicating reduced migratory capacity. (**a**) Representative images of wounds at 0, 12, and 24 h (40 × magnification). Red arrows indicate scratch width. Scale bars = 500 µm. (**b**) Denuded wound areas at each time point. (**c**) Quantitative analysis of percentage wound closure relative to 0 h. Data are mean ± SD from three independent biological replicates (n = 3). Statistical significance versus DMSO was determined by Student's t-test. *P < 0.05, **P < 0.001; n.s., not significant.

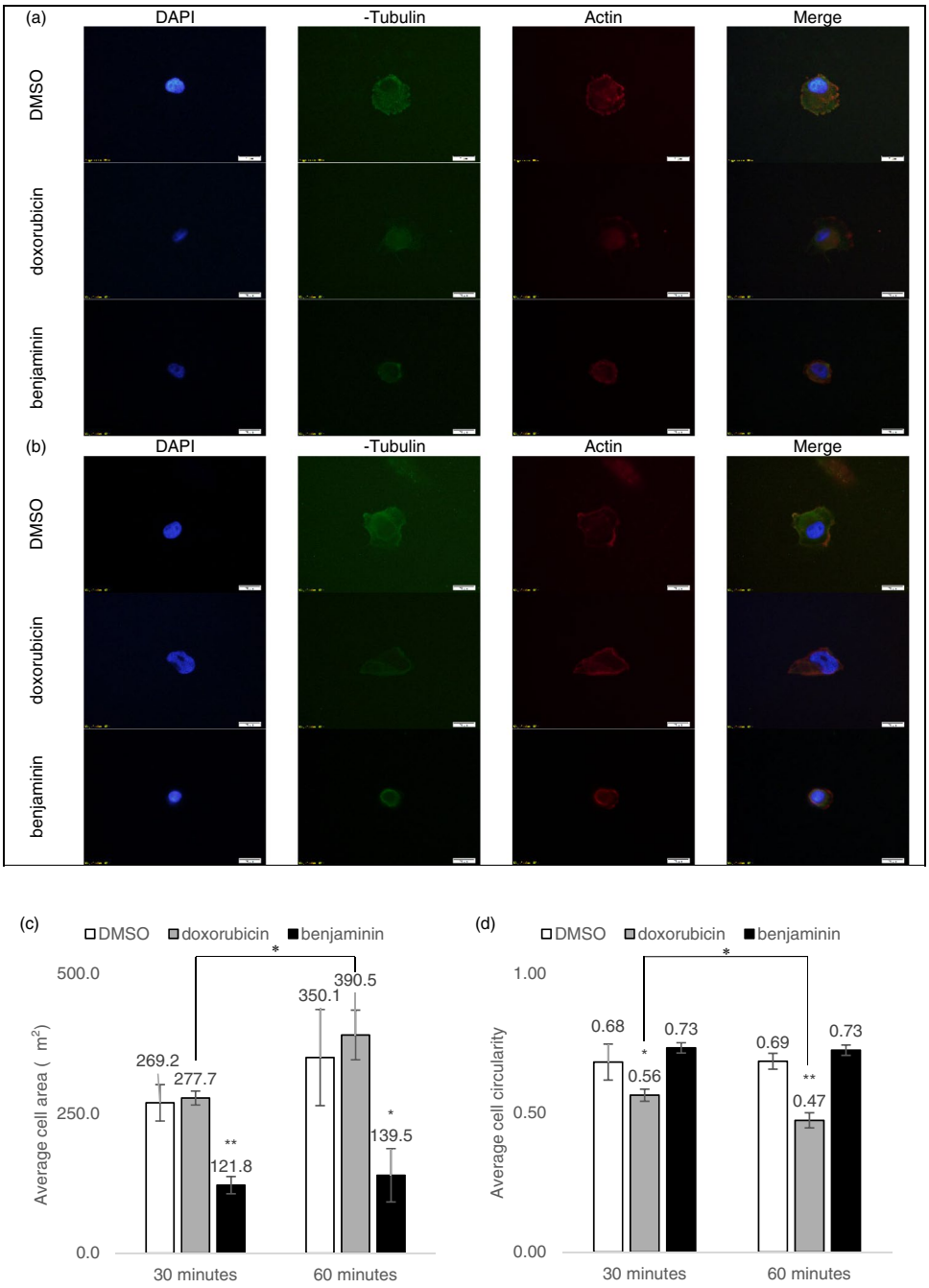

Fig. 6. Effects of treatment on MCF-7 cell spreading. Benjaminin significantly reduced cell area at both time points without affecting circularity, whereas doxorubicin decreased circularity without altering cell area. Only doxorubicin-treated cells exhibited significant time-dependent changes in both parameters. (**a**–**b**) Representative fluorescence images of cell morphology following treatment with 0.1% DMSO (control), benjaminin (IC_{50}), or doxorubicin (IC_{50}) for 30 and 60 min. (**c**) Quantitative analysis of cell area. (**d**) Quantitative analysis of cell circularity. Data are presented as mean ± SD from three independent biological replicates (n = 3). Statistical significance was determined using one-way ANOVA with Dunnett's post-hoc test. *P < 0.05, **P < 0.001.

epithelial cells. These results indicate a degree of tumour selectivity and support the potential of benjaminin as a multi target anticancer candidate. The observed effects on cell cycle progression, cytoskeletal organisation, and apoptotic signalling suggest coordinated disruption of tumour associated processes. However, the underlying mechanisms were not directly established in this study. As the work is limited to in vitro models, further mechanistic validation, subtype specific evaluation, and in vivo studies are required to determine the translational potential of benjaminin in breast cancer.

Data availability

The datasets supporting the conclusions of this study are included within the article and its supplementary materials.

Received: 7 January 2026; Accepted: 27 April 2026
Published online: 23 May 2026

References

1. Arnold, M. et al. Current and future burden of breast cancer: Global statistics for 2020 and 2040. *Breast* **66**, 15–23 (2022).
2. Ferlay, J. et al. Global Cancer Observatory: Cancer Today. https://gco.iarc.who.int/today (2024).
3. Morgan, E. et al. Metastatic recurrence in women diagnosed with non-metastatic breast cancer: A systematic review and meta-analysis. *Breast Cancer Res.* **26**, 171 (2024).
4. Swanton, C. et al. Embracing cancer complexity: Hallmarks of systemic disease. *Cell* **187**, 1589–1616 (2024).
5. Marvalim, C., Datta, A. & Lee, S. C. Role of p53 in breast cancer progression: An insight into p53 targeted therapy. *Theranostics* **13**, 1421–1442 (2023).
6. Kim, J.-H. et al. Occurrence of p53 gene abnormalities in gastric carcinoma tumors and cells lines. *JNCI J. Natl. Cancer Inst.* **83**, 938–943 (1991).
7. Innocenti, M. (2018) New insights into the formation and the function of lamellipodia and ruffles in mesenchymal cell migration. *Cell Adh. Migr.* https://doi.org/10.1080/193369181448352 (2018).
8. Jhaveri, K. & Marmé, F. Current and emerging treatment approaches for hormone receptor-positive/human epidermal growth factor receptor 2-negative metastatic breast cancer. *Cancer Treat. Rev.* **123**, 102670 (2024).
9. Zhang, J. et al. Natural products and derivatives for breast cancer treatment: From drug discovery to molecular mechanism. *Phytomedicine* **129**, 155600 (2024).
10. Stevens, P. F. A revision of the Old World species of *Calophyllum* (Guttiferae). *J. Arnold Arbor.* **61**, 117–699 (1980).
11. Gómez-Verjan, J. C., Rodríguez-Hernández, K. D. & Reyes-Chilpa, R. Bioactive Coumarins and Xanthones From Calophyllum Genus and Analysis of Their Druglikeness and Toxicological Properties. *Stud. Natl. Prod. Chem.* https://doi.org/10.1016/B978-0-444-63930-1.00008-9 (2017).
12. Kilus, M., Abdul Samad, N. & Daud, S. A review of the effects of *Calophyllum* spp. on cancer cells. *J. Angiother.* **7**, 1–6 (2023).
13. Jin, L. et al. Antiproliferative and proapoptotic activity of GUT-70 mediated through potent inhibition of Hsp90 in mantle cell lymphoma. *Br. J. Cancer* **104**, 91–100 (2011).
14. Gómez-Verjan, J. C. et al. Network Pharmacology Uncovers Anticancer Activity of Mammea-Type Coumarins from Calophyllum brasiliense. *Planta Med.* **85**, 14–23 (2019).
15. Mah, S. H., Teh, S. S., Ismail, A. A. F. & Ee, G. C. L. Anti-proliferative Effects of a Coumarin Benjaminin on Four Human Cancer Cell Lines. *Pharm. Sci. Res.* **7**, 7 (2020).
16. Sahimi, M. S., Daud, A. G., Teh, S., See, S. S. & Sukari, I. A new natural product compound Benjaminin from Calophyllum benjaminum. *Pertanika J. Trop. Agric. Sci* **38**, 1–6 (2015).
17. Mohidin, T. B. M. & Ng, C. C. (2015) BARF1 gene silencing triggers caspase-dependent mitochondrial apoptosis in Epstein-Barr virus-positive malignant cells. *J. Biosci.* **40**, 41–51 (2015).
18. Qin, Y. et al. Epigenetic silencing of miR-137 induces drug resistance and chromosomal instability by targeting AURKA in multiple myeloma. *Leukemia* **31**, 1123–1135 (2017).
19. Banka, S. et al. Activating *RAC1* variants in the switch II region cause a developmental syndrome and alter neuronal morphology. *Brain* **145**, 4232–4245 (2022).
20. Slocik, J. M., Dennis, P. B., Kuang, Z., Pelton, A. & Naik, R. R. Creation of stable water-free antibody based protein liquids. *Commun. Mater.* **2**, 118 (2021).
21. Daodu, O. B. et al. Assessment of antibody assay methods in determination of prevalence of infectious bursal disease among local chickens and guinea fowls in Kwara state, North Central Nigeria. *Vet. World* **11**, 1183 (2018).
22. Kciuk, M. et al. Doxorubicin—An agent with multiple mechanisms of anticancer activity. *Cells* **12**, 659 (2023).
23. Landry, P., Rousseau, A.-M. & Skalli, L. Adverse Effects of Antipsychotics. *Clin. Trials Psychopharmacol.: A Better Brain: Second Edn.* https://doi.org/10.1002/9780470749180.ch17 (2010).
24. Linders, A. N. et al. A review of the pathophysiological mechanisms of doxorubicin-induced cardiotoxicity and aging. *npj Aging* **10**, 1–9 (2024).
25. Comşa, Ş, Cîmpean, A. M. & Raica, M. The story of MCF-7 breast cancer cell line: 40 years of experience in research. *Anticancer Res.* **35**, 3147 (2015).
26. Vale, N. et al. Normal breast epithelial MCF-10A cells to evaluate the safety of carbon dots. *RSC Med. Chem.* **12**, 245–253 (2021).
27. Manríquez-Torres, JdeJ. et al. Isolation and cytotoxic activity of phyllocladanes from the roots of *Acacia schaffneri* (Leguminosae). *Molecules* **25**, 3944 (2020).
28. Kishk, S. M. et al. Design and synthesis of coumarin derivatives as cytotoxic agents through PI3K/AKT signaling pathway inhibition in HL60 and HepG2 cancer cells. *Molecules* **27**, 6709 (2022).
29. Gao, P. et al. Alteration of cyclin D1 in gastric carcinoma and its clinicopathologic significance. *World J. Gastroenterol.* **10**, 2936–2939 (2004).
30. Grillo, M. et al. Validation of cyclin D1/CDK4 as an anticancer drug target in MCF-7 breast cancer cells: Effect of regulated overexpression of cyclin D1 and siRNA-mediated inhibition of endogenous cyclin D1 and CDK4 expression. *Breast Cancer Res. Treat.* **95**, 185–194 (2006).
31. Ramadan, M. F. Fig (Ficus carica): Production, processing, and properties. https://doi.org/10.1007/978-3-031-16493-4 (2023).
32. Chaudhry, G.-S., Md Akim, A., Sung, Y. Y. & Sifzizul, T. M. T. Cancer and apoptosis: The apoptotic activity of plant and marine natural products and their potential as targeted cancer therapeutics. *Front. Pharmacol.* **13**, 842376 (2022).
33. Zhao, X. et al. Design, synthesis and biological evaluation of plant-derived miliusol derivatives achieve TNBC profound regression in vivo. *Eur. J. Med. Chem.* https://doi.org/10.1016/j.ejmech.2024.116882 (2024).
34. Barnum, K. J. & O'Connell, M. J. Cell cycle regulation by checkpoints. *Methods Mol. Biol.* **1170**, 29–40 (2014).
35. Thu, K. L., Soria-Bretones, I., Mak, T. W. & Cescon, D. W. Targeting the cell cycle in breast cancer: Towards the next phase. *Cell Cycle* **17**, 1871–1885 (2018).
36. Todd, M. C., Langan, T. A. & Sclafani, R. A. Doxycycline-regulated p16MTS1 expression suppresses the anchorage-independence and tumorigenicity of breast cancer cell lines that lack endogenous p16. *J. Cancer* **8**, 190 (2017).
37. Wang, J. et al. Aberrant Cyclin D1 splicing in cancer: from molecular mechanism to therapeutic modulation. *Cell Death Dis.* **14**, 244 (2023).
38. Ma, N., Xu, E., Luo, Q. & Song, G. Rac1: A regulator of cell migration and a potential target for cancer therapy. *Molecules* **28**, 2976 (2023).
39. Fusté, N. P. et al. Cytoplasmic Cyclin D1 regulates cell invasion and metastasis through the phosphorylation of paxillin. *Nat. Commun.* **7**, 11581 (2016).

40. Nössing, C. & Ryan, K. M. 50 years on and still very much alive: 'Apoptosis: A basic biological phenomenon with wide-ranging implications in tissue kinetics'. *Br. J. Cancer* **128**, 426–431 (2023).
41. Danforth, D. N. & Zhu, Y. Conversion of Fas-resistant to Fas-sensitive MCF-7 breast cancer cells by the synergistic interaction of interferon-gamma and all-trans retinoic acid. *Breast Cancer Res. Treat.* **94**, 81–91 (2005).
42. Zeng, L. et al. Death Receptor 6 induces apoptosis not through Type I or Type II pathways, but via a unique mitochondria-dependent pathway by interacting with Bax protein. *J. Biol. Chem.* **287**, 29125–29133 (2012).

Acknowledgements
The authors sincerely thank Universiti Teknologi MARA (UiTM), Jengka, Pahang, for their support and for providing the benjaminin compound used in this study. Appreciation is also extended to the Breast Cancer Translational Research Program (BCTRP@PKTAAB), Pusat Kanser Tun Abdullah Ahmad Badawi, Universiti Sains Malaysia.

Author contributions
MK: Investigation, Formal analysis, Data curation, Visualisation, Writing – Original Draft, Writing – Review & Editing. SD: Resources, Supervision. NMA: Supervision, Writing – Review & Editing, Validation. JJ: Validation. GCLE: Resources. NAS: Conceptualization, Methodology, Validation, Resources, Supervision.

Declarations

Competing interests
The authors declare no competing interests.

Additional information
Supplementary Information The online version contains supplementary material available at https://doi.org/10.1038/s41598-026-51303-6.

Correspondence and requests for materials should be addressed to N.A.S.

Reprints and permissions information is available at www.nature.com/reprints.

Publisher's note Springer Nature remains neutral with regard to jurisdictional claims in published maps and institutional affiliations.